

Characterization of the Microdomain Structure in Polystyrene–Polyisoprene Block Copolymers by ^1H Spin Diffusion and Small-Angle X-ray Scattering Methods

Kevin S. Jack,[†] Jiahu Wang,[†] Almeria Natansohn,^{*,†} and Richard A. Register[‡]

Department of Chemistry, Queens University, Kingston, Ontario, Canada K7L 3N6, and
Department of Chemical Engineering, Princeton University, Princeton, New Jersey 08544

Received September 30, 1997; Revised Manuscript Received February 23, 1998

ABSTRACT: ^1H spin diffusion and small-angle X-ray scattering (SAXS) measurements were carried out for a series of polystyrene–polyisoprene block copolymers of varying molecular weight and molecular architecture. The sizes of domains and the thickness of the interphase in the copolymers were determined from the spin diffusion measurements using a model which explicitly considers the effects of ^1H spin–lattice relaxation. The thickness of the interphase determined by NMR was found to be constant (ca. 3 nm) for all of the copolymers. The variations in domain size and intersphere distance as a function of molecular weight were found to be in good agreement with those determined by the more established SAXS methods. However, the intersphere distances measured by NMR were found to be consistently smaller than those measured by SAXS, and this difference may be caused by simplifications in the morphological model used in the analysis of the spin diffusion curves.

Introduction

Multiphase polymeric materials are of considerable commercial value to the polymer industry. Much attention has been devoted to characterizing and controlling the microdomain structure of multiphase polymers, as it is well-known that the desired mechanical properties of these materials are intimately associated with the microdomain structures adopted by the materials. As the size of the domains approaches that of the molecular level, it becomes increasingly difficult to accurately quantify the microdomain structures in these materials. A number of experimental techniques are commonly used to characterize the microdomain structure of multiphase polymers close to the molecular level, e.g., transmission electron microscopy (TEM), small-angle X-ray scattering (SAXS), small-angle neutron scattering (SANS), fluorescence spectroscopy, and solid-state NMR spectroscopy. Each of these techniques, however, has its own advantages and disadvantages, and it is useful to employ a number of techniques to unambiguously characterize the microdomain structure of a polymeric material.

Measurements of ^1H spin diffusion by solid-state NMR spectroscopy have proven to be an extremely powerful technique for characterizing the microdomain structures of multiphase polymers. Recent examples of investigations of the microdomain structure of semicrystalline polymers,^{1,2} polymer blends,^{3–5} block copolymers,^{6–9} and core–shell latexes^{10–12} can be found in the literature. The power of this technique lies in its ability to probe both the size of domains and the thickness of the interphase between domains and in the fact that no modification of the sample is required to obtain these measurements. The latter point is of crucial importance if one is interested in investigating

the effect of processing conditions on the microdomain structure of the polymer. One of the limitations of this technique, however, is that the reliability of the dimensions of the microdomain structure obtained from these measurements is not well established. Moreover, the development of spin diffusion methods for determining the microdomain structure of polymers is currently an active field of research, see e.g. references 1, 5, 9, 10, and 13–15, and the full power and limitations of these methods have yet to be realized.

Direct measurements of ^1H spin diffusion are obtained by monitoring the redistribution of ^1H magnetization within a multiphase polymer system, following the creation of a spatially inhomogeneous distribution of magnetization.^{5,16} Approximate theories for extracting domain sizes from ^1H spin diffusion curves measured for two-phase polymer systems (i.e. systems in which no interphase exists) have been proposed,^{5,7} however, quantitative measurements of the size of domains and interfacial thickness in multiphase polymer systems can only be obtained by simulations of the experimental diffusion curves.^{1,5,7,14}

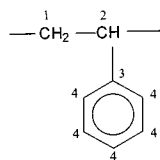
Very recently, this research group¹³ and Kenwright and Say⁹ have shown that the accuracy with which the microdomain structure can be determined from spin diffusion curves can be greatly improved by including ^1H spin–lattice relaxation terms in simulations of ^1H spin diffusion. In particular it has been shown that microdomain structure measurements obtained from a model which does not include spin–lattice relaxation can lead to an overestimation of the thickness of the interfacial region.¹³ In this work the microdomain structure of a series of polystyrene–polyisoprene (SI) block copolymers of varying molecular weights and molecular architectures is investigated by measurements of ^1H spin diffusion using a model which explicitly treats ^1H T_1 relaxation, and by SAXS measurements. When the results obtained from the NMR measure-

[†] Queens University.

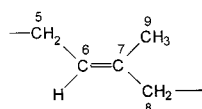
[‡] Princeton University.

Table 1. Molecular and Morphological Characteristics of Block Copolymers Studied

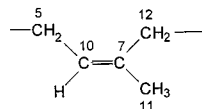
sample code	total M_w (kg/mol)	w_s	v_s (23 °C)	q^* (nm ⁻¹)	R (nm)	D (nm)	a (nm)
SI 8/54	62.6	0.130	0.114	0.256	8.3	30.1	34.7
SI 11/68	78.4	0.135	0.119	0.224	9.6	34.4	39.7
SI 12/79	90.6	0.131	0.115	0.207	10.3	37.2	42.9
SIS 8/104/8	120.1	0.130	0.114	0.242	8.8	31.8	36.7
SIS 10/129/10	149.0	0.130	0.114	0.217	9.8	35.5	40.9

Chart 1

Poly(styrene)



Trans-1,4 Polyisoprene



Cis-1,4 Polyisoprene

ments are compared with those obtained from the more established SAXS measurements, the reliability of the spin diffusion model developed recently in our laboratory¹³ is further demonstrated.

Experimental Section

Materials. The synthesis and characterization of the di- and triblock copolymers studied here has been described previously.¹⁷ Compositions were determined by ¹H NMR in solution, and molecular weights were determined by gel permeation chromatography, correcting for the known compositions through the method of Tung.¹⁸ These results are summarized in Table 1. Polydispersity indexes were less than 1.03 for all six specimens. Each polymer is indicated by the block architecture, followed by the molecular weight of each block in kg/mol; e.g., SIS 10/129/10 denotes a triblock copolymer containing styrene–isoprene–styrene blocks of 10, 129 and 10 kg/mol, respectively. The polystyrene weight fractions (w_s) determined by ¹H NMR were converted to polystyrene volume fractions (v_s), as listed in Table 1, using the known densities of polyisoprene¹⁹ and polystyrene²⁰ at 23 °C ($\rho_I = 0.9048$ g/cm³; $\rho_s = 1.0479$ g/cm³). S and I homopolymers were obtained from Aldrich and Polymer Sources, respectively. The molecular weights of these polymers are shown in Table 1. Furthermore, the diene microstructure of I is similar (ca. 90% 1,4-addition) to that of the isoprene in the block copolymers. The chemical structures of S and I are shown in Chart 1.

Samples for SAXS measurements were first heated to temperatures between the polystyrene block glass transition and the order–disorder transition temperature (T_{ODT}) for sufficient time to develop a well-ordered structure, as described previously.²¹ NMR measurements for two of the copolymers (SI 12/79 and SI 10/129/10) were collected from samples in both the well ordered and metastable, or disordered, states. It was found that the presence (or absence) of long-range order of the domains in the copolymers did not affect the NMR measurements reported here. The NMR measurements for the remaining copolymers were, therefore, obtained from samples that were not heat treated.

SAXS. Small-angle X-ray scattering measurements were made using a compact Kratky camera²² and hot stage²¹ described previously. Data correction procedures, including slit length desmearing, were as previously described.²² The SAXS data always exhibited sharp peaks in a q ratio of 1: $\sqrt{2}$:

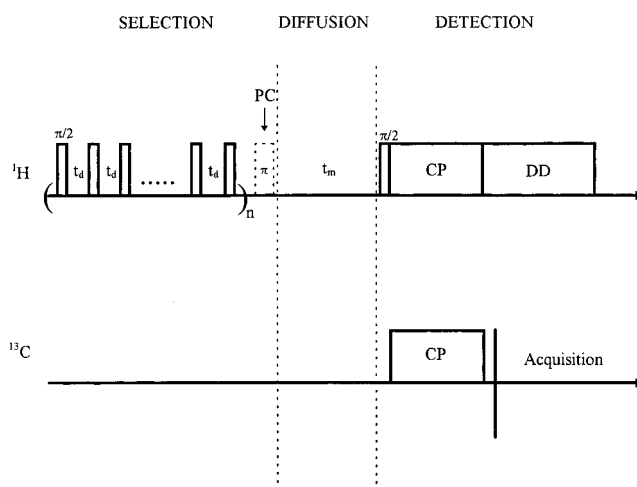


Figure 1. Schematic representation of the dipolar filter pulse sequence. For the experiments performed in this work $t_d = 16$ μ s and $n = 7$. PC represents the phase alternation used to suppress T_1 relaxation effects. CP and DD represent cross-polarization and dipolar decoupling, respectively.

$\sqrt{3}$, where $q = (4\pi/\lambda)\sin \theta$; λ is the wavelength of the Cu K α radiation, and θ is half the scattering angle. Representative data can be found in ref 21; these peak positions are as expected for a body-centered-cubic packing of minority-phase spheres, which we infer to be the equilibrium morphology for our materials.^{23,24} Samples were then cooled to room temperature and their SAXS patterns recorded. The position of the leading-order peak in the room-temperature pattern, q^* , is given in Table 1 for each material. As noted previously,²¹ the change in q^* on passing through the order–disorder transition is negligibly small in these materials, so the sphere radii and intersphere distances calculated below can also be considered as good approximations to the metastable structure observed in the specimens at room temperature prior to annealing,²¹ though no long-range order is present.

¹³C NMR Spectroscopy. ¹³C CPMAS NMR spectra were collected on a Bruker ASX-200 spectrometer, operating at 50.3 MHz. Spin-locking field strengths of 64 kHz ($\pi/2$ pulse time = 3.9 μ s), cross-polarization times of 1 ms, and MAS spinning rates of 3.3 kHz were used in the acquisition of all of the ¹³C NMR spectra reported in this work. ¹H T_1 relaxation times were measured via cross-polarization to ¹³C using an inversion–recovery pulse sequence.

¹H spin diffusion measurements were obtained via cross-polarization to ¹³C using the dipolar filter pulse sequence,²⁵ shown schematically in Figure 1. A gradient of ¹H magnetization is initially created by the “selection” portion of the pulse sequence which consists of 12 $\pi/2$ pulses (3.9 μ s pulse time) separated by short delays. Seven repetitions of the first 12 pulses of the pulse sequence and an interpulse delay of 16 μ s were used to completely eliminate the ¹H NMR signal due to the more rigid S domain. For each mixing time, ca. 3000 transients were collected with a recycle delay of 2 s. Errors due to small changes in experimental conditions (e.g. fluctuations in the tuning characteristics of the probe) during the spin diffusion experiments were minimized by collecting the NMR signal for each mixing time in blocks of 128 transients.

Simulated ¹H Spin Diffusion Curves. Simulated ¹H spin diffusion curves were obtained using a model, developed in our laboratory, which considers the effects of both ¹H spin diffusion and ¹H spin–lattice relaxation on the distribution of magnetization, as described very recently.¹³ The morphological model used for all of the simulations of ¹H spin diffusion consisted of a three-dimensional simple cubic lattice of S cubes surrounded by a mixed SI phase (interphase) which are dispersed in a continuous I matrix, as shown schematically in Figure 2A. The composition of the interphase was assumed to vary linearly across the interphase. The only variable parameters in the model are the size of the S domains (d_s)

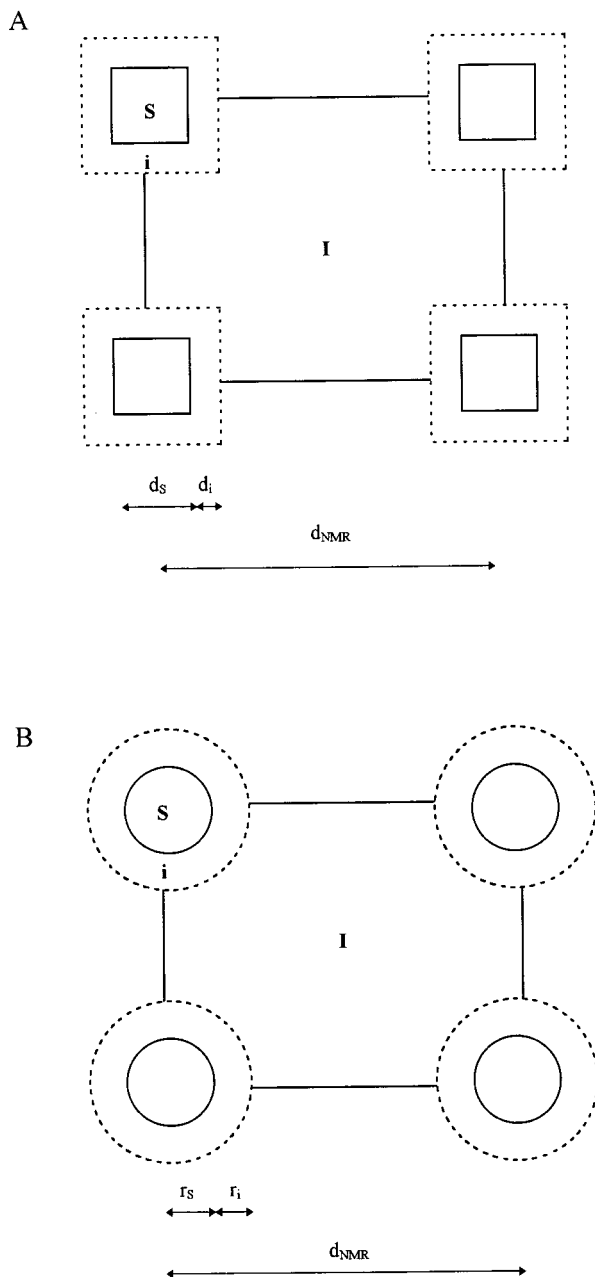


Figure 2. Schematic representations of the three-phase morphological models considered for the SI copolymers. This figure shows two-dimensional representations of three-dimensional models. Simulations were performed assuming A), a simple cubic (sc) model (A), which was then transformed to an equivalent model (B) containing spherical S domains. Note that each S domain is surrounded by six nearest neighbors at a distance d_{NMR} .

and the thickness of the interphase (d_i), and the following nonvariable parameters were used for all of the simulations.

1. The proton concentrations of the S and I domains were calculated to be 0.081 and 0.107 g cm⁻³, respectively, from the known densities and formula weights of the homopolymers.

2. The diffusion coefficient used for S (0.8 nm² ms⁻¹) is the same as that determined by Clauss et al.⁷ The diffusion coefficient for I (0.05 nm² ms⁻¹) was assumed to be the same as that reported for polybutadiene at room temperature²⁶ and the diffusion coefficient in the interphase region was assumed to decrease linearly from 0.8 nm² ms⁻¹ at the S boundary to 0.05 nm² ms⁻¹ at the I boundary.

3. The volume fraction of S (v_s) in each of the copolymers is shown in Table 1.

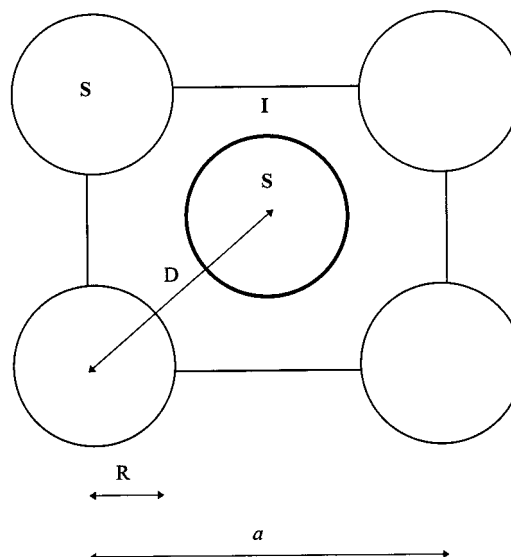


Figure 3. Two-dimensional schematic representation of the two-phase bcc model used in the analysis of the SAXS measurements. Note that each S domain is surrounded by eight nearest neighbors at a distance D .

4. Intrinsic ¹H T_1 relaxation times for S and I were chosen to be equal to the T_1 relaxation times measured for the two homopolymers: 1400 ms and 290 ms for S and I, respectively. Furthermore, the intrinsic relaxation time at any point in the interphase is assumed to be given by

$$\frac{1}{T_1} = \frac{\chi_S^H}{T_1^S} + \frac{\chi_I^H}{T_1^I} \quad (1)$$

where χ_S^H and χ_I^H are the ¹H fractions of S and I, respectively, at some given position in the interphase.

Results and Discussion

SAXS Measurements. From the volume fraction of S (v_s) and the first-order peak position q^* measured by SAXS, sphere radii (R) and intersphere distances (D) can be calculated in the approximation of complete phase separation between the two blocks.²⁷ For a body-centered-cubic structure, the peak at q^* corresponds to the spacing between the (110) planes, which are separated by $a/\sqrt{2}$, where a is the length of the side of the unit cell. The following relations are used:

$$R = (2\pi/q^*)(3v_s/\sqrt{8}\pi)^{1/3} \quad (2)$$

$$D = \sqrt{6}\pi/q^* \quad (3)$$

$$a = \sqrt{8}\pi/q^* \quad (4)$$

Values of R , D , and a are given in Table 1 for each of the six polymers. A schematic representation of the microdomain structure parameters R , D , and a is shown in Figure 3.

NMR Measurements. ¹³C NMR. ¹³C CPMAS spectra of S, I, and a S–I diblock copolymer (sample SI 12/79) are shown in Figure 4. The peak assignments shown on this figure correspond to the numbering system used in Chart 1. The weak, unlabeled resonances observed in the CPMAS spectrum of I at 18.9, 48.2, and 112.0 ppm can be ascribed to 3,4-addition. It can be seen from Figure 4 that there are nonoverlapping resonances in the CPMAS spectra of S and I, which can

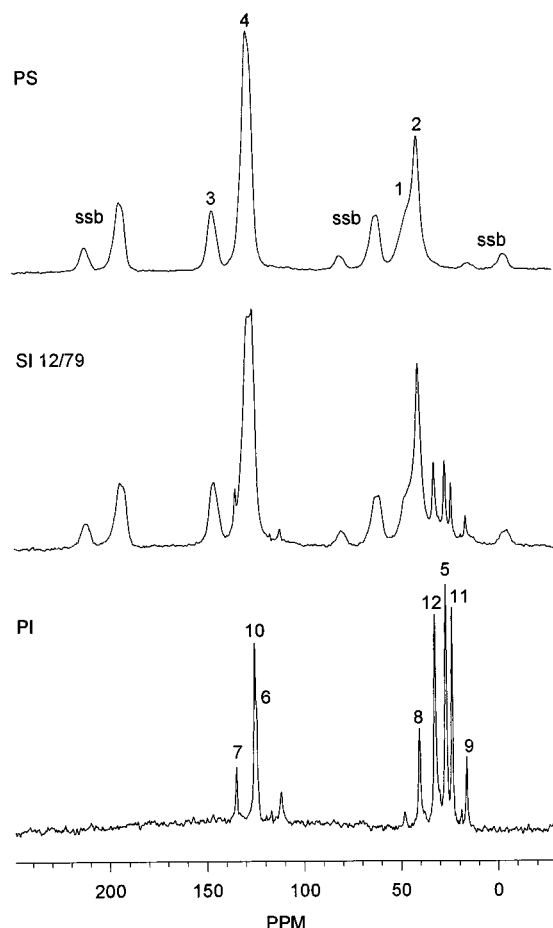


Figure 4. CPMAS spectra of S, I, and SI 12/79 copolymer. The numbers are assignments for the carbons shown in Chart 1. Spinning sidebands in the CPMAS spectrum of S are denoted by ssb.

Table 2. ^1H T_1 Relaxation Times Measured for S, I, and SI Copolymers

sample code	^1H T_1 of S block (ms)	^1H T_1 of the I block (ms)
S	1400	
I		290
SI 8/54	430	380
SI 11/68	460	360
SI 12/79	370	320
SIS 8/104/8	430	380

be used to probe the magnetization in S and I blocks of the copolymers: e.g., the nonprotonated aromatic resonance of S at 145 ppm and the resonances due to the methylene carbons of I at 26 ppm.

^1H T_1 Relaxation Time Measurements. ^1H T_1 relaxation times measured for pure S, pure I, and the S–I copolymers are presented in Table 2. It can be seen from this table that the ^1H T_1 relaxation times of S and I in the copolymers are almost completely averaged by ^1H spin diffusion. Qualitatively, it can be inferred from this averaging, and previously established theories in the literature, that the upper limit for the size of domains in the S–I block copolymers is on the order of a few tens of nanometers.^{28,29} In this work, however, we are primarily concerned with the quantitative analysis of the microdomain structure of polymeric materials. To achieve this goal, NMR measurements of ^1H spin diffusion in the copolymers and detailed simulations of spin diffusion were obtained and are reported below.

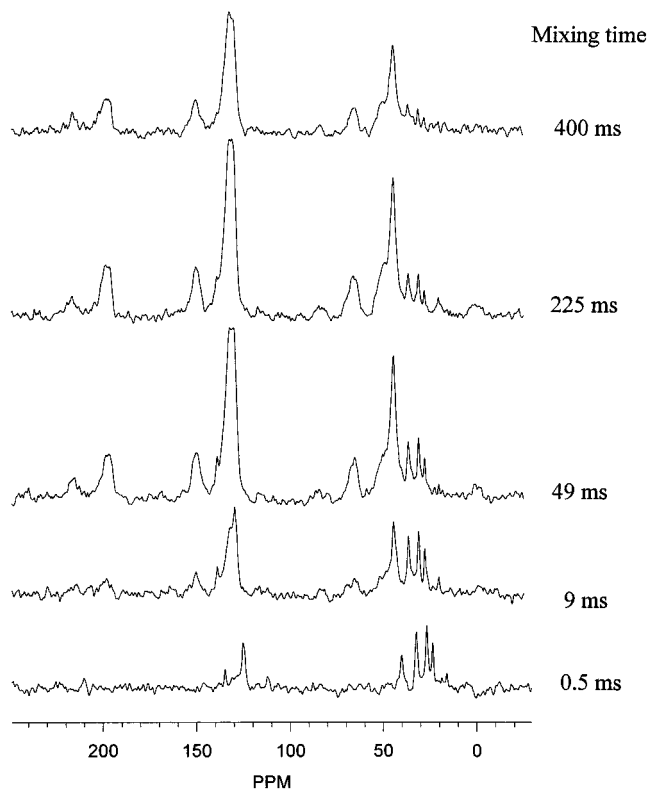


Figure 5. Dipolar filter spectra obtained for SI 12/79 copolymer at the various mixing times (t_m) shown on the figure.

^1H Spin Diffusion Measurements. Solid-state NMR measurements of ^1H spin diffusion were used to characterize the microdomain structure of the SI copolymers. Good reviews of the historical aspects, theories and practical details pertaining to the measurement of ^1H spin diffusion in multiphase polymers can be found in the literature.^{1,5,16} A brief description of the dipolar filter experiments used in this work is provided below. The dipolar filter pulse sequence²⁵ was chosen to obtain ^1H spin diffusion measurements in SI block copolymers as it is arguably the simplest and most suitable method for obtaining these measurements in systems comprised of a rigid domain (S) and a soft domain (I).

A typical ^1H spin diffusion experiment obtained using the dipolar filter pulse sequence for the SI 12/79 copolymer is presented in Figure 5. The dipolar filter pulse sequence (see Figure 1) can be conveniently separated into three parts: (1) the initial selection of magnetization in the more mobile domains, by elimination of magnetization in the rigid domains, to generate a nonequilibrium distribution of magnetization; (2) the diffusion of ^1H magnetization from the initially selected mobile domains to the rigid domains during a mixing time t_m , i.e., the recovery from the nonequilibrium state to the equilibrium distribution of magnetization; and (3) the indirect detection of the ^1H magnetization after a given mixing time (t_m) by cross-polarization to ^{13}C nuclei.

It can be seen from the spectrum collected with the shortest mixing time in Figure 5 that the initial selection portion of the dipolar filter completely eliminates the ^1H magnetization in the rigid (S) domains in the copolymer; i.e., the spectrum is similar to that of pure I. The recovery of ^1H magnetization in the S domain in the copolymer, due to ^1H spin diffusion from the I domain, can clearly be seen from the spectra collected

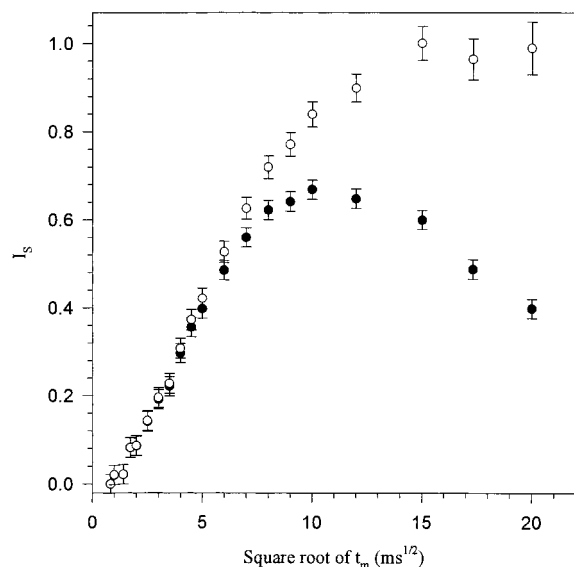


Figure 6. Raw (filled circles) and corrected (open circles) ^1H spin diffusion curves measured for the SI 12/79 copolymer. The corrected curve was obtained by multiplying each point in the raw curve by $\exp(t_m/T_1)$. The error bars were estimated from the random noise in the dipolar filter spectra.

with mixing times >0.5 ms, as is evident by the increases in the ^{13}C NMR peaks ascribed to S. If one compares the spectra collected with a mixing times of 225 ms or greater with the CPMAS spectrum of SI shown in Figure 4, it can also be seen that complete recovery of the equilibrium distribution of ^1H magnetization is achieved in this time. By comparison with previously published measurements of ^1H spin diffusion in multiphase polymers, this observation suggests that the sizes of the S domains in this copolymer are on the order of a few tens of nanometers.^{7,8,30}

Finally it is pertinent to point out the decrease in magnetization observed for all peaks in the dipolar filter experiment when the mixing time is increased from 225 to 400 ms. This decrease in intensity is inherently related to the phase alternation used to reduce the effects of T_1 relaxation on the measured spin diffusion curves. As previously discussed in the literature,^{7,16} the form of the reduction in the measured signal intensity is given by $\exp(t_m/T_1^\delta)$; where t_m is the mixing time and T_1^δ is the ^1H spin-lattice relaxation time in the laboratory frame for the resonance being measured. Quantitative analysis of spin diffusion curves obtained with this phase alternation have normally been carried out^{6,8,12,16,30} after the measured signal intensity has been corrected for this exponential reduction factor. However, if the effects of T_1 relaxation are explicitly treated in the simulations of ^1H spin diffusion, then such corrections are no longer necessary.^{9,13} This final point is discussed in further detail below.

To quantify the size of microdomain structure in the SI copolymers, the recovery of the ^1H magnetization in the S domain of the copolymers is measured as a function of the square root of the mixing time ($\sqrt{t_m}$); the so-called " ^1H spin diffusion curve". A typical ^1H spin diffusion curve measured for the SI 12/79 sample is shown in Figure 6. The curve defined by the filled circles in Figure 6 was obtained by plotting the intensity of the S contribution to the peak at 127 ppm as a function of $\sqrt{t_m}$ and has not been corrected for the loss in signal intensity due to the phase alternation used to reduce T_1 effects. As can be seen from Figure 4, the

peak in the ^{13}C CPMAS spectrum of SI at 127 ppm contains contributions from both S and I domains of the copolymer. The contribution of the S domain to this peak was calculated as

$$I_S = I_{127} - f I_{26} \quad (5)$$

where I_{127} and I_{26} are the intensities of the ^{13}C resonances at 127 and 26 ppm respectively, and f is the ratio of I_{127}/I_{26} in the dipolar filter spectrum of SI copolymer obtained immediately after selection, i.e., without a mixing time. The ^1H spin diffusion curve shown in Figure 6 is quantitatively similar to that which is obtained by plotting the intensity of the nonprotonated aromatic peak at 145 ppm as a function of $\sqrt{t_m}$ (not shown here). The only difference between the two methods is that the curve obtained directly from the ^{13}C peak at 145 ppm contains more noise than that obtained from the peak at 127 ppm, due the large difference in intensity of the two peaks (see e.g. the CPMAS spectrum of pure S). This observation was true for all of the SI copolymers studied in this work.

As discussed above, the phase alternation (PC pulse in Figure 1) used to reduce the effects of T_1 relaxation also gives rise to a reduction in the overall intensity of the magnetization measured. The form of this reduction is given by: $\exp(t_m/T_1^\delta)$; where t_m is the mixing time and T_1^δ is the ^1H spin lattice relaxation time measured from the peak at 127 ppm. This reduction in signal intensity can be seen most clearly in the spin diffusion curve defined by the filled circles in Figure 6. In the past, ^1H spin diffusion curves have normally been reported after the intensity of each point in the raw curve has been corrected by multiplying by $\exp(t_m/T_1^\delta)$. The corrected ^1H spin diffusion curve measured for the SI 12/79 copolymer has been included in Figure 6 (open circles) so that the reader may compare this work with previously published spin diffusion measurements more easily. It should be noted that both of the spin diffusion curves shown in Figure 6 contain identical information about the microdomain structure of the copolymer. Correction of the diffusion curve is not necessary as long as a diffusion model which explicitly treats ^1H T_1 relaxation is used to simulate the spin diffusion curves; as is used in this work. Moreover, the use of the raw spin diffusion curve in the determination of the microdomain structure is more convenient because it is simpler and the correction leads to an amplification of the absolute uncertainties at large mixing times.

^1H spin diffusion curves measured for the SI 12/79 and SI 8/54 diblock copolymers are presented in Figure 7. These curves have not been multiplied by the exponential factor due to phase alternation and each curve is scaled such that the maximum intensity is equal to 1. It can be seen from this figure that as the molecular weight of the copolymer increases from 62 to 90 K, the spin diffusion curve initially rises more slowly, reaches a maximum at a longer value of $\sqrt{t_m}$, and decreases at a slower rate as the mixing time is further increased. To show this trend more clearly, the differences between the spin diffusion curves (SI 12/79 – SI 8/54) are also shown in Figure 7.

Simulation of ^1H Spin Diffusion Curves. Quantitative measurements of the microdomain structure, i.e., the size of domains and interphases, of multiphase polymers by measurements of ^1H spin diffusion have previously been demonstrated by a number of authors, see for example,^{1,5,13,16,25} For polymers which are com-

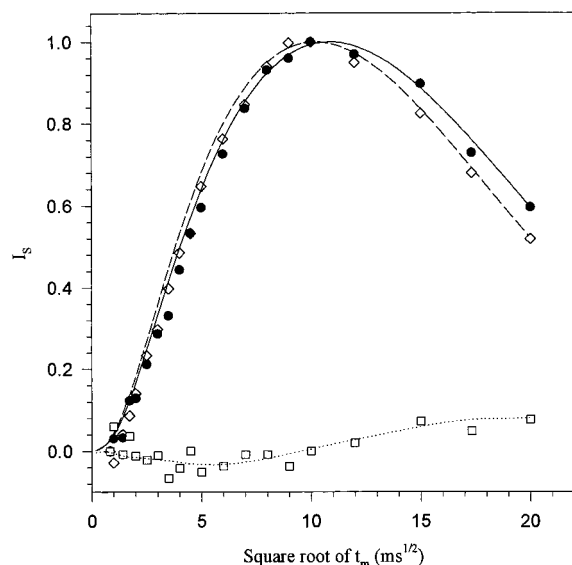


Figure 7. ^1H spin diffusion curves measured for the SI 12/79 (circles) and SI 8/54 (diamonds) diblock copolymers. The best possible simulations for these copolymers are represented by the solid and dashed lines, respectively. The differences ($I_{\text{SI } 12/79} - I_{\text{SI } 8/54}$) between the experimental data (squares) and simulations (dotted line) for the two copolymers are also shown.

prised of two pure phases, it has been shown that the size of the minor component domains can be determined directly from the measured spin diffusion curve, by extrapolating the initial linear portion of the diffusion curves; the so-called initial rate approximation.⁷ However, the presence of a significant amount of an interphase, i.e., a region of gradual change in composition between the two pure phases, has been shown to reduce the rate of spin diffusion at short mixing times, leading to a characteristic sigmoidal shape in the measured spin diffusion curve.^{5,14,16,25} In such cases, quantification of the microdomain structure of these polymers can only be achieved through simulations of the measured ^1H spin diffusion curves. The initial increase in magnetization of the spin diffusion curves for the SI copolymers shows a significant deviation from linearity for all of the samples; see Figure 7. Simulations of ^1H spin diffusion were, therefore, used to quantify the microdomain structure of the copolymers.

The simulations of ^1H spin diffusion which include spin-lattice relaxation effects used in this work have previously been described in detail, in the literature.¹³ The combined processes of spin diffusion and spin-lattice relaxation in the copolymers are described by

$$\frac{\partial c(r, t_m)}{\partial t} = D(r) \Delta c(r, t_m) + \frac{c^\infty - c(r, t_m)}{T_1(r)} \quad (6)$$

where $c(r, t_m)$, $D(r)$, and $T_1(r)$ are the specific spin magnetization, the spin diffusion coefficient, and the spin-lattice relaxation time, respectively, at any position (r) and time (t_m) in the copolymer. Simulations of ^1H spin diffusion were performed by solving a discrete version of Equation 6, numerically, for $c(r, t_m)$, using the proper boundary conditions¹⁴ and the initial conditions described below. The total spin magnetization $\{M^S(t_m)\}$ in any region (Ω) of the copolymer can be conveniently obtained by integrating the specific spin magnetization $\{c(r, t_m)\}$ over the region of interest. Simulated ^1H spin diffusion curves in this work were obtained by plotting

Table 3. Phase Structure of SI Copolymers Measured by NMR

sample code	d_s (nm \pm 0.8 nm)	d_i (nm \pm 1 nm)	d_{NMR} (nm \pm 2.2 nm)	r_s (nm \pm 0.5 nm)	r_i (nm \pm 1.0 nm)	r' (nm) ^a
SI 8/54	8.5	2.5	23.5	5.6	3.1	7.1
SI 11/68	10.2	2.4	27.0	6.3	3.0	8.2
SI 12/79	11.9	2.1	30.1	7.4	2.6	9.1
SIS 8/104/8	9.0	2.4	24.6	5.6	3.0	7.4
SIS 10/129/10	10.5	2.5	27.5	6.5	3.1	8.3

^a r' is calculated as $r' = (3v_s d_{\text{NMR}}^3 / 4\pi)^{1/3}$, where v_s = volume fraction of S (see Table 1).

the total spin magnetization of S in the copolymer $\{M^S(t_m)\}$ as a function of $\sqrt{t_m}$.

For a given set of microdomain structure parameters (d_s and d_i), two separate simulations have been carried out using different initial conditions: one corresponding to the spin magnetization of the system immediately after the application of the dipolar filter and the other corresponding to the magnetization of the system immediately after a π pulse (PC pulse shown in Figure 1) is applied, following the dipolar filter. In the former case, the initial magnetization in the selected (I) region was taken to be 1 and that in the suppressed (S) region to be 0; where 1 represents total magnetizations of the protons in this domain and 0 represents total suppression of proton magnetization. For the latter simulation, the initial magnetization for I and S are chosen to be -1 and 0 , respectively. The differences of magnetization in the S (or I) region from the above two simulations are easily formed by subtraction of the second simulation from the first and they are directly comparable with the experiment data obtained using phase alternation.

The initial magnetization in the interfacial region of the copolymers was set to 0 for all of the simulations presented here. Simulations in which an initial gradient of magnetization was allowed to exist in the interface were also performed. It was found, however, that any magnetization that is initially allowed to exist in the interface leads to a significant offset in the spin diffusion curve because it is necessary, in the numerical simulations, to treat the interface as a single chemical species (i.e. intimately mixed S-I) whose composition and properties vary in a linear fashion. That is, any magnetization in the I chains at time 0 undergoes instantaneous equilibration with the S chains after the first time step. A significant offset was also observed in simulations in which an, arbitrarily chosen, linear weighting function was applied to the intensity of magnetization of the S chains in the interface, to allow for a possible reduction in the contribution to the measured ^{13}C signal intensity due to a poorer CP efficiency of the S chains in this region. Although this offset in the spin diffusion curves is an artifact of the numerical simulations, in reality one might expect the initial magnetization of the I chains in the interface to equilibrate with the S chains in a time⁴ on the order of 1–2 ms. This equilibration would lead to an initial rapid increase in the measured spin diffusion curve and is not consistent with what is observed in Figure 7, i.e., an initial slow build-up of magnetization.

To determine the microdomain structure from the simulations of ^1H spin diffusion, the S domain size (d_s) and the interfacial thickness (d_i) have been independently varied, and the set which leads to the best fit between experiment and simulation is reported in Table 3. The uncertainty in each of the parameters reported

in Table 3 was estimated from the fitting procedure, i.e., simulations using parameters outside of this range were considered to provide poor fits to the experimental data. These uncertainties do not reflect systematic errors associated with the choice of the model used in the simulation, which affect the absolute scaling of the microdomain structural parameters. These errors are discussed separately in this paper (see below). Definitions of the microdomain structure parameters d_s , d_i , and d_{NMR} are shown in Figure 2A. Furthermore, the best simulated spin diffusion curves for the SI 12/79 and 8/54 diblock copolymers are presented in Figure 7. It can be seen from this figure that the agreement between the simulated and experimental diffusion curves is very good, for all of the copolymers. Specifically, it can be seen that the simulations catch the essential features of the experimentally measured spin diffusion curves, i.e., the initial slow increase in magnetization at short mixing times, the subsequent attainment of a maximum, and finally the decrease in magnetization for mixing times $> \text{ca. } 100 \text{ ms}$ ($10 \text{ ms}^{1/2}$). Such an extent of decrease in magnetization cannot be predicted by a pure spin diffusion model, i.e., one that does not contain ^1H T_1 relaxation terms.

Discussion of the Microdomain Structure of SI Copolymers. It can be seen by comparing Figures 2A and 3 that there are some differences between the models that were used to determine the microdomain structure of the SI copolymers from the SAXS and NMR measurements. For the SAXS investigation the model used consists of a two-phase (i.e. no interfacial region), body-centered-cubic (bcc) arrangement of S spheres in a I matrix. As mentioned above, the choice of a bcc arrangement is consistent with previous literature.^{21,23,24,27} Both theory^{31–33} and experiment^{34,35} indicate that there should be a substantial degree of interfacial mixing in these SI block copolymers.^{36,37} In principle, it is possible to extract information on the interfacial thickness from analysis of the tail of the SAXS curve (Porod analysis), and this approach has previously been applied to block copolymers.^{36,37} However, the necessary background subtraction can impart a large uncertainty to the interfacial thickness so derived,^{34,38} and we have not attempted such an analysis here. In contrast with the model used for the SAXS measurements, the morphological model used in the simulation of the NMR results consists of a simple cubic (sc) arrangement of S cubes in a I matrix. Although a bcc arrangement of S spheres is thought to better describe the true morphology of the SI copolymers, it was not possible to simulate ^1H spin diffusion curves using such a model because of the computational time is prohibitively long at present. Moreover, the NMR model contains three phases: a pure S domain, a mixed SI phase or interfacial region (whose composition is assumed to vary linearly with distance from the S boundary to the I boundary), and a pure I domain. Indeed it is not possible to adequately simulate the early time behavior of the spin diffusion curves using a simple two-phase model for the morphology of the copolymers.

To compare the microdomain structure of the copolymers as determined by SAXS and by NMR, the domain sizes determined from the NMR measurements are transformed to equivalent spherical dimensions. The cubic S domains are converted to spherical domains of equal volume using

$$r_s = \sqrt[3]{\frac{3}{4\pi}} d_s \quad (7)$$

where r_s is the radius of the spherical S domains and d_s is the cubic S domain size determined by NMR. Similarly, the thickness of the interphase (d_i) can be approximately converted to spherical units (r_i) keeping the volume of the interphase constant. A schematic representation of the microdomain structure parameters r_s , r_i , and d_{NMR} is shown in Figure 2B, and the values for the S sphere radii (r_s) and intersphere distances (d_{NMR}) for the copolymers are shown in Table 3.

In Figure 8 the size of S domains determined by both NMR and SAXS and the thickness of the interfacial region determined by NMR for each of the SI diblock copolymers is plotted as a function of the total molecular weight of the copolymer. The trends in the size of S domains in the copolymers as a function of molecular weight measured by NMR and SAXS are in good agreement. As discussed above, the number of phases used in the determination of the domain sizes by NMR and SAXS are different. It is expected, therefore, that the S particle size measured by NMR (r_s), using a three-phase model of the morphology, will be smaller than those measured by SAXS (R), using a two-phase model, because R will also encompass some fraction of the interfacial region; compare Figures 2B and 3. For each of the copolymers, the size of the hypothetical sphere (r') which has a volume equal to the sum of that occupied by S in the pure-S and interfacial regions of the copolymer has been calculated and tabulated in Table 3 and is also shown in Figure 8. It can be seen from this figure that, qualitatively, the agreement between r' and R is very good. Quantitatively, however, the NMR measurements of the hypothetical S spheres (r') are ca. 14–20% smaller than those measured by SAXS (R). This discrepancy between the two sets of measurements is believed to be due to the use of an approximate sc lattice model in the simulation of the spin diffusion curves. A discussion of the quantitative differences between the NMR and SAXS measurements of the microdomain structure, including other possible sources of error, is presented below.

From Figure 8 it can also be seen that an interphase (r_i) of ca. 2.9 nm was measured by NMR for each of the SI diblock copolymers and that the thickness of the interfacial region was found to remain constant for the range of molecular weights investigated here. The latter observation is consistent with the theory of Helfand and Wasserman,^{31–33} which predicts that the interphase thickness in the copolymers is determined by the interaction parameter of the homopolymers and the mer length and is independent of the molecular weight. The thickness of the interphase measured in these copolymers is in agreement with that previously measured in SI copolymers using SANS,³⁴ SAXS,^{36,37} and NMR relaxation time measurements.³⁵ From Porod analysis of SAXS curves for lamellar³⁷ and spherical³⁶ SI diblocks based on I containing a low content of 1,4-addition, Hashimoto and co-workers determined that the interfacial thickness, assuming a linear gradient of composition, measured ca. 2 nm. A value of ca. 2.2 nm was obtained by Richards and Thomason for SI diblocks containing I with a high content of 1,4-addition. In the work of Richards and Thomason the thickness of the interphase was determined using Porod analysis of SANS data, wherein the background subtraction can be

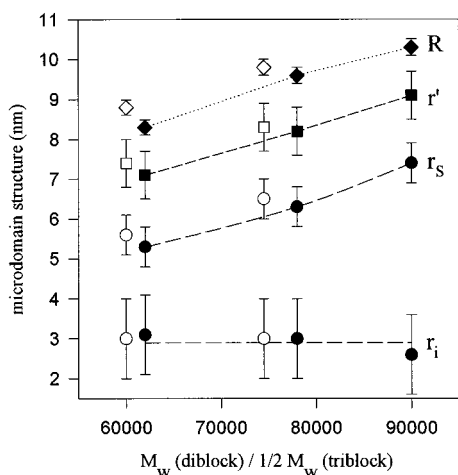


Figure 8. Phase structure of the SI copolymers as measured by NMR (circles) and SAXS (diamonds). Note that the SI diblock copolymers (filled symbols) are plotted as a function of the total molecular weight of the copolymer, while the symmetrical SIS triblock copolymers (open symbols) are plotted as a function of $1/2 M_w$. The squares represent the hypothetical two-phase S domain sizes calculated from the NMR measurements.

made with greater certainty compared with SAXS data.³⁴ Both groups found that the interfacial thickness was independent of molecular weight, as predicted by theory.^{31–33} Tanaka and Nishi³⁵ have also measured the thickness of the interphase in a SIS triblock copolymer by deconvoluting the ^1H FID of this sample into three components, which are assigned to S, interfacial, and I domains. From the fractions of each of these components and the intersphere distance measured by TEM, the thickness of the interface in this sample was determined to be ca. 2.6 nm.

The microdomain structure parameters for the two symmetric triblock SIS copolymers, as measured by NMR and SAXS, are plotted as a function of half of the total molecular weight of the copolymers in Figure 8. It can be seen from this figure that the morphology of each symmetric triblock (SIS) copolymer is similar to that of a diblock (SI) copolymer of half of the total molecular weight. This similarity in morphology is observed in both the NMR and SAXS measurements and has also been reported in a previous SAXS investigation of SI copolymers.^{27,37,39}

To further verify the reliability of the NMR measurements of the microdomain structure, the intersphere distances measured by SAXS and NMR for each of the copolymers are presented in Figure 9. In contrast with the size of domains determined by the two techniques, the intersphere distances can be considered to be independent of the number of phases chosen for the morphological model used in the determination of the microdomain structure. It can be seen from this figure that both NMR and SAXS show the same trends in the intersphere distance as a function of the molecular weight of the copolymer. Indeed the power law exponent (α) for the three diblock copolymers, determined from the double-logarithmic plot, from SAXS measurements ($\alpha = 0.58$) and NMR ($\alpha = 0.66$) are in agreement with each other and the two-thirds power law relationship predicted theoretically^{31–33} and measured experimentally by Hashimoto et al.³⁶ As noted by Clauss et al.⁷ the value of α determined from the NMR experiments is independent of any absolute calibration im-

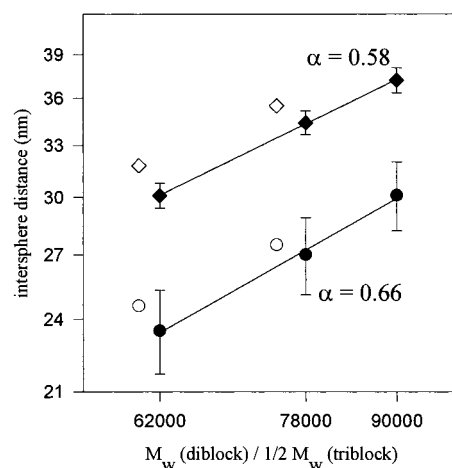


Figure 9. Double logarithmic plot of the intersphere distances measured by NMR (d_{NMR} , circles) and SAXS (D , diamonds). α is the exponent of the power law relationship for the SI diblocks (filled symbols). SIS triblocks (open symbols) are plotted as a function of $1/2 M_w$.

posed on the NMR measurements through the choice of diffusion coefficients. The agreement between the NMR and SAXS measurements, therefore, provides evidence for the sensitivity of the NMR technique to detect differences in the microdomain structure of the copolymers.

It can also be seen from Figure 9 that the intersphere distances determined by SAXS are consistently larger than those determined by NMR. Furthermore, calculations of the intersphere distances using the equilibrium thermodynamic theory of Helfand^{31–33} were found to be in reasonable agreement with those measured by SAXS. Although the intersphere distance is independent of the number of phases used in the morphological model, this distance does depend on the packing arrangement used in the calculation of D (bcc model, see eq 3) or in the simulations of ^1H spin diffusion (sc model, see point 3 in the Experimental Section above). It is possible, using simple geometric considerations, to calculate a hypothetical intersphere distance (d'_{NMR}) between neighboring particles of S plus interfacial material (radius = $r_s + r_i$) assuming a bcc ordered arrangement of these particles:

$$d'_{\text{NMR}} = \frac{\sqrt[3]{2} \sqrt{3}}{2} d_{\text{NMR}} \quad (8)$$

That is, this hypothetical bcc lattice has the same volume fraction of S as the sc lattice used in the simulations of ^1H spin diffusion. This transformation, however, does not account for the effect of the packing arrangement on the measured ^1H spin diffusion curve. Furthermore, it should be noted that, the ratio d'_{NMR}/D is equal to r'/R (see Figure 8) and that d'_{NMR} is, therefore, ca. 14–20% smaller than D . Therefore, while d'_{NMR} is quantitatively closer to D than d_{NMR} , a systematic discrepancy remains.

The differences between the NMR and SAXS measurements may be traced to two possible source; these are as follows.

1. This source is due to an incorrect choice of the diffusion coefficients. It has previously been demonstrated that the domain sizes, and hence the intersphere distance determined from ^1H spin diffusion measurements, is approximately proportional to the square root

of the diffusion coefficient.^{5,7,16} An underestimation in D_S and/or D_I would, therefore, lead to an underestimation in the intersphere distances determined from the simulation of the experimental spin diffusion curves. Clauss et al.⁷ have measured ^1H spin diffusion curves for polystyrene-poly(methyl methacrylate) (S-PMMA) block copolymers which have been characterized by TEM and SAXS, and which span a large range of molecular weights. From this investigation D_S was determined to be $0.8 \text{ nm}^2 \text{ ms}^{-1}$ (used in this work), assuming that the diffusion coefficients of the glassy S and PMMA domains were equal. Spin diffusion coefficients in highly mobile polymers, however, have not been well investigated. The only experimental investigation of diffusion coefficients in mobile polymers known to us has been published by Spiegel et al.²⁶ The spin diffusion coefficients of polybutadiene (B) at three different temperatures were determined by comparison of NMR and TEM measurements of a single S-B block copolymer, although the effects of ^1H T_1 relaxation were not considered in the analysis of the spin diffusion curves. It was shown that the spin diffusion coefficient of B is not a simple linear function of the ^1H line width, as predicted by Abragam.⁴⁰ The value of $D_I = 0.05 \text{ nm}^2 \text{ ms}^{-1}$ used here was chosen to be the same as that determined for B at 297 K. From the glass transition temperature (ca. 218 K) and the ^1H line width (ca. 100 Hz) of the I blocks in the S-I copolymers reported here and those reported for the B ($T_g \sim 238 \text{ K}$, ^1H line width $\sim 150 \text{ Hz}$) blocks in the work of Spiegel et al.,²⁶ the diffusion coefficient for I would be expected to be slightly smaller than that of B, assuming similar ^1H concentrations. An overestimation of D_I , however, would lead to an overestimation in the microdomain structural parameters determined by NMR, not the underestimation observed.

2. This source is due to the use of an approximate lattice in the simulations of ^1H spin diffusion. Due to the limitation of the available computational power, the simulations were carried out by employing a sc lattice rather than a bcc lattice as determined by SAXS. In a sc lattice, each dispersed-phase domain has six nearest neighbors, whereas in a bcc lattice, a dispersed domain is surrounded by eight nearest neighbors. Therefore, given equivalent volume fractions of the dispersed phase (see eq 8), the spin diffusion process will be less efficient in a sc lattice than in a bcc lattice. Consequently, the use of the approximate sc lattice in the simulation of the experimental ^1H spin diffusion curve leads to an underestimation of the intersphere distance.

It is possible to calibrate the spin diffusion coefficient for one of the components of the copolymer from the SAXS measurements. For example, if it is assumed that the value of D_S is correct then D_{NMR} can be forced to equal D (measured from SAXS), if a value of $D_I = 0.08 \text{ nm}^2 \text{ ms}^{-1}$ is used to simulate the ^1H spin diffusion curves, assuming a sc lattice. Such a calibration, however, cannot be justified until the errors associated with the use of the approximate lattice can be eliminated.

Conclusions

Solid-state NMR measurements of ^1H spin diffusion and SAXS were used to investigate the microdomain structure of a series of SI di- and triblock copolymers which have well-defined molecular weights. Simulations of ^1H spin diffusion using a model which considers

^1H spin-lattice relaxation were employed in the analysis of the NMR measurements.¹³ It was found that the quality of the simulations that could be achieved by including ^1H T_1 terms into the model were very good for all of the copolymers investigated, and that the corresponding microdomain structure parameters obtained from these simulations are, therefore, more accurate than those obtained from pure spin diffusion models. To determine the reliability of these microdomain structure measurements, the NMR measurements were compared with SAXS measurements performed on the same samples. Very good agreement was found between the trend in the size of domains and the intersphere distances as a function of the molecular weight for the copolymers. A direct comparison of the intersphere distances measured by SAXS and NMR was undertaken, and it was found that the NMR measurements were consistently smaller than SAXS. It is believed that this discrepancy is caused, at least in part, by the choice of a simple cubic model to represent the morphology of the copolymers, which have previously been shown to adopt a bcc microdomain structure. It was not possible to perform simulations using a bcc model because of the computational expense of such a model. We are currently investigating methods for performing these simulations in the future.

Acknowledgment. The block copolymers used in this work were generously provided by Dr. Gary Marchand of Dow Chemicals/Dexco Polymers. The authors also thank Daniel Quiram and Chiajen Lai for assistance with the SAXS measurements. This research was funded in part by the Environmental Science and Technology Alliance of Canada (ESTAC) and the Natural Sciences and Engineering Research Council (NSERC) of Canada. We thank both NSERC and ESTAC for their financial support. Support for the work at Princeton was provided by the National Science Foundation, Polymers Program, through Grants DMR-9257565 and DMR-9711436.

References and Notes

- (1) Demco, D. E.; Johansson, A.; Tegenfeldt, J. *Solid State NMR* **1995**, *4*, 13.
- (2) Eckman, R. R.; Henrichs, P. M.; Peacock, A. J. *Macromolecules* **1997**, *30*, 2474.
- (3) VanderHart, D. L.; Manley, R. S. J.; Barnes, J. D. *Macromolecules* **1994**, *27*, 2826.
- (4) VanderHart, D. L. *Macromolecules* **1994**, *27*, 2837.
- (5) VanderHart, D. L.; McFadden, G. B. *Solid State NMR* **1996**, *7*, 45.
- (6) Cho, G.; Natansohn, A.; Ho, T.; Wynne, K. J. *Macromolecules* **1996**, *29*, 9, 2563.
- (7) Clauss, J.; Schmidt-Rohr, K.; Spiess, H. W. *Acta Polym.* **1993**, *44*, 1.
- (8) Cai, W. Z.; Schmidt-Rohr, K.; Egger, N.; Gerharz, B.; Spiess, H. W. *Polymer* **1993**, *34*, 267.
- (9) Kenwright, A. M.; Say, B. J. *Solid State NMR* **1996**, *7*, 85.
- (10) Landfester, K.; Boeffel, C.; Lambla, M.; Spiess, H. W. *Macromolecules* **1996**, *29*, 5972.
- (11) Spiegel, S.; Landfester, K.; Lieser, G.; Boeffel, C.; Spiess, H. W.; Eidam, N. *Macromol. Chem. Phys.* **1995**, *196*, 985.
- (12) Landfester, K.; Spiess, H. W. *Macromol. Rapid Commun.* **1996**, *17*, 875.
- (13) Wang, J.; Jack, K. S.; Natansohn, A. *J. Chem. Phys.* **1997**, *107*, 1016.
- (14) Wang, J. *J. Chem. Phys.* **1996**, *104*, 4850.
- (15) Idiytullin, D. S.; Khozina, E. V.; Smirnov, V. S. *Solid State NMR* **1996**, *7*, 17.
- (16) Schmidt-Rohr, K.; Spiess, H. W. *Multidimensional Solid-State NMR and Polymers*; Academic Press: London, 1994; pp 402–439 and references therein.

- (17) Adams, J. L.; Graessley, W. W.; Register, R. A. *Macromolecules* **1994**, *27*, 6026.
- (18) Tung, L. H. *J. Appl. Polym. Sci.* **1979**, *24*, 953.
- (19) Nemoto, N.; Moriwaki, M.; Odani, H.; Kurata, M. *Macromolecules* **1971**, *4*, 215.
- (20) Richardson, M. J.; Savill, N. G. *Polymer* **1977**, *18*, 3.
- (21) Adams, J. L.; Quiram, D. J.; Graessley, W. W.; Register, R. A.; Marchand, G. R. *Macromolecules* **1996**, *29*, 2929.
- (22) Register, R. A.; Bell, T. R. *J. Polym. Sci., Polym. Phys.* **1992**, *30*, 569.
- (23) Bates, F. S.; Cohen, R. E.; Berney, C. V. *Macromolecules* **1982**, *15*, 589.
- (24) Leibler, L. *Macromolecules* **1980**, *13*, 1602.
- (25) Egger, N.; Schmidt-Rohr, K.; Blumich, B.; Domke, W.-D.; Stapp, B. *J. Appl. Polym. Sci.* **1992**, *44*, 289.
- (26) Spiegel, S.; Schmidt-Rohr, K.; Boeffel, C.; Spiess, H. W. *Polymer* **1993**, *34*, 4566.
- (27) Sakurai, S.; Kawada, H.; Hashimoto, T.; Fetters, L. J. *Macromolecules* **1993**, *26*, 5796.
- (28) Chu, C. W.; Dickinson, L. C.; Chien, J. C. W. *J. Appl. Polym. Sci.* **1990**, *41*, 2311.
- (29) Asano, A.; Takagoshi, K.; Hikichi, K. *Polymer* **1994**, *35*, 5630.
- (30) Cho, G.; Natansohn, A. *Can. J. Chem.* **1994**, *72*, 2255.
- (31) Helfand, E.; Wasserman, Z. R. *Macromolecules* **1976**, *9*, 879.
- (32) Helfand, E.; Wasserman, Z. R. *Macromolecules* **1978**, *11*, 960.
- (33) Helfand, E.; Wasserman, Z. R. *Macromolecules* **1980**, *13*, 994.
- (34) Richards, R. W.; Thomason, J. L. *Polymer* **1983**, *24*, 1089.
- (35) Tanaka, H.; Nishi, T. *J. Chem. Phys.* **1985**, *82*, 4326.
- (36) Hashimoto, T.; Fujimura, M.; Kawai, H. *Macromolecules* **1980**, *13*, 3, 1660.
- (37) Hashimoto, T.; Shibayama, M.; Kawai, H. *Macromolecules* **1980**, *13*, 3, 1237.
- (38) Roe, R. J. *J. Appl. Crystallogr.* **1982**, *15*, 182.
- (39) Hadziioannou, G.; Skoulios, A. *Macromolecules* **1982**, *15*, 258.
- (40) Abragam, A. *The Principles of Nuclear Magnetism*; Oxford: London, 1961; pp 138–139.

MA971436A